Polyphenolic Profiling of Green Waste Determined by UPLC-HDMS E

Potter, Colin M.; Jones, David L.

Processes

DOI:
10.3390/pr9050824

Published: 09/05/2021

Publisher's PDF, also known as Version of record

processes

MDPI

Article

Polyphenolic Profiling of Green Waste Determined by UPLC-HDMS^E

Colin M. Potter [1,*] and David L. Jones [1,2]

[1] Centre for Environmental Biotechnology, School of Natural Sciences, Bangor University, Bangor, Gwynedd LL57 2UW, UK; d.jones@bangor.ac.uk
[2] UWA School of Agriculture and Environment, The University of Western Australia, Perth, WA 6009, Australia
* Correspondence: colinmpotter@gmail.com

Abstract: Valorising green waste will greatly enhance and promote the sustainable management of this large volume resource. One potential way to achieve this is the extraction of high value human health promoting chemicals (e.g., polyphenols) from this material. Our primary aim was to identify the main polyphenols present in four contrasting green waste feedstocks, namely *Smyrnium olusatrum*, *Urtica dioica*, *Allium ursinum* and *Ulex europaeus*, using UPLC-HDMS^E. Polyphenol-rich *Camellia sinensis* (green tea) was used as a reference material. Samples were extracted and analysed by UPLC-HDMS^E, which was followed by data processing using Progenesis QI and EZ Info. A total of 77 high scoring polyphenolic compounds with reported benefits to human health were tentatively identified in the samples, with abundances varying across the plant types; *A. ursinum* was seen to be the least abundant in respect to the polyphenols identified, whereas *U. europaeus* was the most abundant. Important components with a diverse range of bioactivity, such as procyanidins, (−)-epigallocatechin, naringenin, eriodictyol and *iso*-liquiritigenin, were observed, plus a number of phytoestrogens such as daidzein, glycitin and genistein. This research provides a route to valorise green waste through the creation of nutritional supplements which may aid in the prevention of disease.

Keywords: TWIMS; polyphenols; phenol-explorer database; UPLC-MS-MS; Synapt G2-Si; phenolomics

Citation: Potter, C.M.; Jones, D.L. Polyphenolic Profiling of Green Waste Determined by UPLC-HDMS^E. *Processes* **2021**, *9*, 824. https://doi.org/10.3390/pr9050824

Academic Editor: Ibrahim M. Abu-Reidah

Received: 10 April 2021
Accepted: 6 May 2021
Published: 9 May 2021

1. Introduction

In most countries, green waste typically represents a high volume, low value resource, with most of this material being composted and subsequently spread back to agricultural land to improve soil quality [1]. However, green waste also represents a promising starting material for the direct extraction of valuable compounds and for the chemical and fermentative conversion of this waste into basic chemicals [2]. One of the main issues in valorising this resource, however, is knowledge of what high value products can be obtained in sufficient quantities from different types of green wastes to make it commercially viable. One area that has drawn particular interest has been the extraction of polyphenols [3]. These plant species may also contain many other non-polyphenolic bioactive chemicals which are also worthy of attention. Co-extraction of these would, of course, further enhance the value of waste materials, though this research was focused on polyphenols. A full cost–benefit analysis and life cycle assessment are required to determine the valorisation benefits relative to other synthesis or extraction procedures.

Polyphenols are a naturally occurring group of secondary metabolites which are relatively abundant in plants and which are purported to have many health benefits [4–6]. For example, they are thought to play an important role in disease prevention, resulting not only from their antioxidant ability but also their epigenetic influence and their positive impact on the composition of gut microbiota. Due to their complex chemical structures, many of these plant-derived bioactive polyphenols can be difficult to synthesize in large quantities [7]. Green waste offers a potentially cheap feedstock to extract and purify these

compounds; however, this necessitates good knowledge of the polyphenols present in different source materials [2].

Green waste is expected to contain many thousands of chemicals. Consequently, high resolution analytical approaches are needed to enable separation and identification of the myriad chemicals present. One potential solution is the use of ultra-performance liquid chromatography (UPLC) linked to an ion mobility time-of-flight high-definition/high-resolution mass spectrometer (UPLC-HDMS^E). Recent work characterising phenolic compounds in forestry waste has shown that UPLC-HDMS^E can provide an in-depth analysis of the wide suite of phenolics present [8]. This is also supported by the use of UPLC-HDMS^E for the detection and characterisation of bioactive compounds in complex medicinal mixtures and urine [9,10]. The characterisation of polyphenolics in agricultural or municipal green waste via UPLC-HDMS^E has not, to the best of our knowledge, been previously undertaken. The aim of this study was therefore to analyse the diversity of polyphenols in four contrasting but common green waste materials generated in municipal or agricultural settings. These plant-based feedstocks have previously been characterised by a range of analytical techniques, but they have not been subject to the potential benefits of the detailed characterisation provided by UPLC-HDMS^E. As a broad reference material, green tea (*Camellia sinensis*) was also included in the study. The phenolic chemistry of this plant material has been well characterised [6,11,12], and can therefore act as a validation of this discovery workflow, i.e., the expected polyphenols associated with green tea should be observed.

2. Materials and Methods

2.1. Sample Collection

Representative samples of Alexanders (*Smyrnium olusatrum*), Stinging Nettle (*Urtica dioica*), Wild garlic (*Allium ursinum*) and Gorse (*Ulex europaeus*) were collected from the Lligwy Bay area of Anglesey, Wales, UK (53°21′14″ N, 4°15′47″ W) in April 2019. The sample of *U. europaeus* was separated into separate flower and stem samples in order to observe whether there were any significant differences in the characterisation of these two physically connected structures. These plants were chosen due to their contrasting phylogenies and their frequent presence in municipal and agricultural green waste streams.

2.2. Sample Preparation

After collection, each sample was thoroughly washed in LC-MS grade water (Optima) and then freeze-dried (48 h) before being ground to a fine powder. A total of 0.5 g of powder was then placed in a glass beaker containing 10 mL of ethanol and sonicated in an ultrasonic water bath for 30 min before being left to stand for 24 h at 4 °C before being sonicated again for a further 30 min. After the solids had settled out, the supernatant was transferred to a polypropylene tube and centrifuged (10,000 rev min^{-1}, 30 min). Through heating to 60 °C, the resultant ethanol solution of extracted components was concentrated to 1 mL; that is to say that 1 mL of extract was equivalent to 1 g of initial sample. The sample produced was stored at −20 °C. The plant samples were prepared in quadruplicate.

2.3. Analytical Instrumentation

HDMS^E mode is a data-independent acquisition in which data for all gas phase parent ions, and also fragments (product ions) created, are recorded. This was recorded and saved as continuum data. In addition, a drift cell was used to collect ion mobility data. The Synapt G2-Si (Waters UK, Wilmslow, Cheshire, UK) can be described as a quadrupole time-of-flight mass spectrometer (Q-ToF) which has ion mobility capability added to the ion path. Analytes, which have been separated by the UPLC, were infused into a Z-Spray^{TM} source (Waters UK, Wilmslow, Cheshire, UK). Simultaneously, leucine enkephalin (Tyr-Gly Gly Phe-Leu) was infused via a separate probe, which provided the lock mass data to correct the mass axis drift which occurs during an acquisition. Baffle switching allowed for the selection of which infusion, analyte or lock mass entered the MS.

2.4. UPLC Conditions

A Waters I-class UPLC was used for analyte separation with a Waters Cortecs Shield RP18 (2.7 µm × 2.1 mm × 100 mm, Waters UK, Wilmslow, Cheshire, UK) solid core column installed. This column provides high selectivity for phenolic compounds due to the use of imbedded polar carbamate technology. A guard column of the same stationary phase was used for protection of the analytical column. Water with 0.1% acetic acid in reservoir A and MeOH with 0.1% acetic acid in reservoir B were used as the mobile phase. The flow rate, column temperature and injection volume were 0.5 mL min^{-1}, 40 °C and 1.0 µL, respectively. The starting composition for this eluent was 90% A and 10% B, with a linear change to 1% A with 99% B over the course of 4 min. At the end point, the initial conditions were returned to over a time of 0.2 min.

2.5. Synapt G2-Si Conditions

Negative ion data, in a mass range of 50 to 1200 Da, was acquired using resolution mode. The scan time was 0.2 s, with an average of 3 scans and a mass window of ±0.5 Da. mode. The cone voltage was 40 V. The method was set to acquire the lockmass (leucine enkephalin, 554.2615 Da) at regular intervals (30 s). This was not used for immediate mass correction throughout the run but stored for later use in the data processing phase.

2.6. Data Processing

Progenesis QI software (NonLinear Dynamics Ltd., Newcastle upon Tyne, UK) was used to process these data. An experimental design was chosen (between subjects) by creating individual groups for the various plant extracts, plus one for the reference (green tea) and one group for blank extracts. As this detail has previously been published [8], only a brief overview is provided here. Post deconvolution, a 5 ppm precursor tolerance was used to compare ions to the ChemSpider Polyphenols database [13] using isotope similarity scores above 90%, an elemental composition of C, O, H only and in an silico fragmentation tolerance of 90%. Similarly, filters were used to reveal only analytes with ANOVA p values ≤0.01 and where blanks were the lowest mean, and, also, scores with a value above 40 were selected for further evaluation. Multivariate analysis (MVA) was conducted through the use of EZInfo (Umetrics, Umeå, Sweden). Matlab (MatWorks Inc., Natlick, MA, USA) was used to create the heat map.

3. Results and Discussion

3.1. Bioactive Phenolic Compounds in the Green Waste Extracts

An Excel file in the supplementary materials (plant extracts XL SM v6) provides a detailed summary of the 77 high-scoring components elucidated through this analysis of green waste. Details such as retention time (min.), normalised abundance, drift time (ms) and accurate mass values are provided for parent ions and their main product ions. Very low ANOVA-p and q values are seen, which indicates a false discovery rate (FDR) close to zero. Mass errors of ≤5 ppm are observed in these data, plus scores of over 80 for isotope similarity.

In cases where it was not possible to distinguish analytes from species of the same accurate mass, the various possibilities are listed. Examples of total ion chromatograms (Figures S1–S6) and example molecular structures of the 29 identified components, with scores of 50.0 and above, are shown in Figure S7. Mass spectra (Figure S8) are available in the supplementary materials.

Green tea, which was used as a reference material, exhibited the expected polyphenols generally associated with this plant in the published literature. These include (−)-epigallocatechin, (−)-epigallocatechin gallate, theaflavin and procyanidin (B1, B2, B3 or B4). Another key component of green tea's polyphenol profile, (−)-epicatechin, was also observed at 1.23 min and m/z 289.0732, with an average abundance of score of 38.1, 6782 average abundance, a mass error of 4.8 ppm and very low ANOVA-p and q values (1.31×10^{-8} and 3.47×10^{-9}). A confirmatory product ion at m/z 245.0808, due to the

loss of 44 Da (CH_3CHO), was observed [14]. This added further validity to this discovery method. An abundance profile of (−)-epicatechin across the plant extracts can be seen in the supplementary materials showing the greatest abundance in the green tea extract (Figure S9).

A heat map was created using averaged abundances for each sample type over the 77 identified polyphenol components (Figure 1). This visual overview of polyphenol identifications shows that abundances are higher in *U. europaeus* flower and stem extracts than they are in the extracts of *S. olusatrum*, *U. dioica* and *A. ursinum*. Furthermore, it can be seen that *A. ursinum* leaf has the lowest abundance of the components identified here. It is also noted that individual plant extracts have their own pattern or fingerprint of abundances, with components showing much variation been plant types.

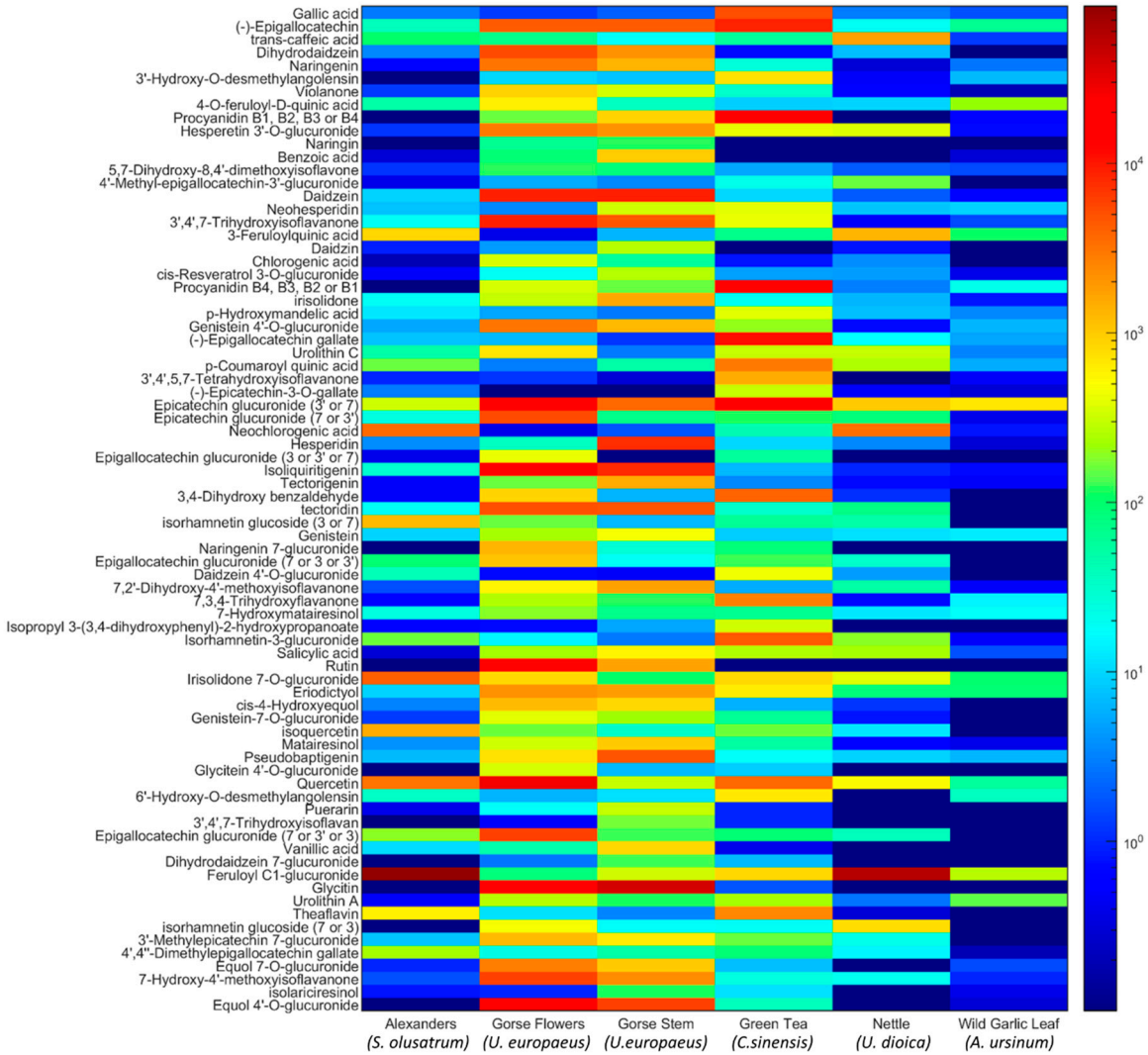

Figure 1. Heat map, using averaged abundances, created for each sample type across the 77 observed polyphenols.

A loadings bi-plot was created as another overview of the data. Pareto scaling was used in this unsupervised principal component analysis (PCA). Sample replicates are tightly clustered and sample types show clear separation. The relationship between sample types and the data swarm of m/z values (x-variables) can also be seen (Figure 2).

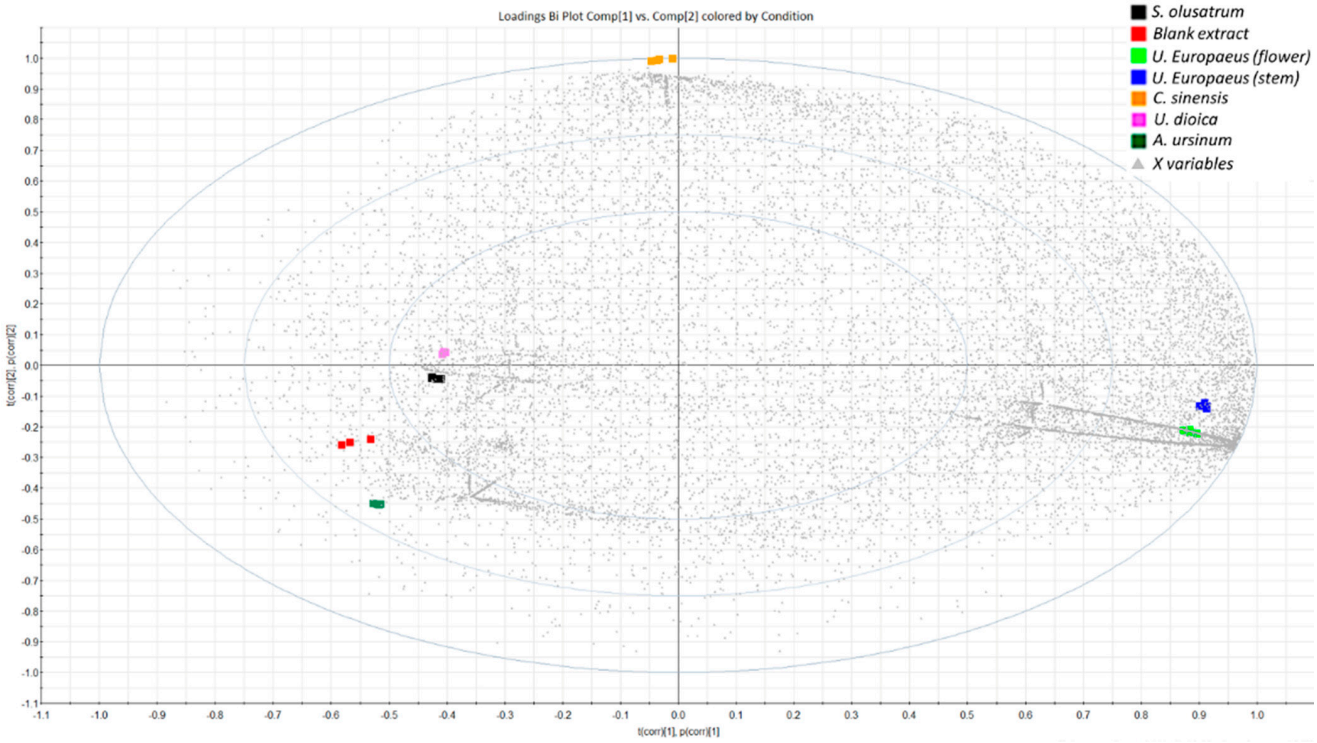

Figure 2. Loadings bi-plot showing tight clustering of sample types within the data swarm.

3.2. Tentative Identification of Polyphenols

Due to the lack of fragmentation data contained in databases, in silico predication has been used here. As the fragmentation mechanisms of polyphenols are well documented, this can be quite an effective approach. Retro-Diels-Alder (RDA) reactions [15] are the general category here, which also applies to the sugar moiety, which is often seen in polyphenols. Additionally, the mass spectra of conjugated phenolic compounds showed the aglycone ion as result of the loss of sugar moieties such as hexosyl ($[M–162]^-$) or pentosyl ($[M–132]^-$). An example of this is seen with the two isomers of isorhamnetin glucoside (3 or 7) that are identified at 1.81 and 2.63 min. Their $[M\text{-}H]^-$ ions undergo the loss of the hexoside moiety to create product ions of m/z 315.0503 and m/z 315.0508. It is also noted that these isobaric species are not only separated by chromatographic retention time but also by drift time, further confirming that these molecules are different in terms of their collision cross section (CCS). The isomer at 1.81 min is seen in high abundance in *U. dioica* and the other isomer at 2.63 min is high in *S. olusatrum*. Both are also fairly abundant in the *U. europaeus* flower extract. Isorhamnetin-3-glucoside is a major component of *Salicornia herbacea*, which is traditionally used in Asian medicine and is thought to exhibit multiple nutraceutical and pharmaceutical properties [16]. Isorhamnetin-7-glucoside is suggested to have antitumour activity in a review of topopoisons from weeds [17].

The highest scoring component, gallic acid, was identified by its $[M\text{-}H]^-$ ion at 1.43 min and the loss of 44 Da to create the product ion m/z 125.0238 $[M\text{-}H\text{-}CH_3CHO]^-$. Although this had an expected high abundance in the green tea extract, it was only present at low abundance in the plant extracts. The identification of (−)-epigallocatechin was achieved by observation of the $[M\text{-}H_2O\text{-}H]^-$ adduct at m/z 287.0562, eluting at 1.41 min and the main MS/MS fragments of m/z 257.0437 $[C_{14}H_{10}O_5\text{-}H]^-$ and m/z 151.0387 $[C_8H_8O_3\text{-}H]^-$. This is one of the key health components of green tea [18] and was present in this extract in high abundance. Although (−)-epigallocatechin was detected in all extracts, it was found to be in particularly high abundance in the *U. europaeus* flower and stem extracts. At m/z 179.0343 and 1.76 min, *trans*-caffeic acid was identified. The product ion m/z 135.0441 $[C_8H_7O_2\text{+e}]^-$ was used for additional confirmation. This component is well

documented in the literature as a potent antioxidant which can aid in the fight against cellular injury due to reactive oxygen species [19], and was present in this study, with the highest abundance being in *U. dioica* and, to a lesser degree, in *S. olusatrum*.

To link together some key phytoestrogens, dihydrodaidzein (CSID154076) was elucidated via its $[M\text{-}H]^-$ adduct (m/z 255.0663) at 1.87 min. Major fragments of m/z 121.0282 $[C_7H_6O_2\text{-}H]^-$ and m/z 119.0495 $[C_8H_8O\text{-}H]^-$ were observed in the high energy MS/MS signal, although other product ions were apparent. Daidzein was observed at 2.58 min and m/z 253.0515, with confirmatory fragments m/z 224.0465 $[C_{14}H_9O_3\text{-}H]^-$ and m/z 208.0520 $[C_{14}H_8O_2\text{+e}]^-$ and genistein eluted at 2.73 min, with a parent ion at m/z 251.0336 $[M\text{-}H_2O\text{-}H]^-$ and primary fragment at m/z 223.0396 $[C_{14}H_{10}O_4\text{-}H_2O\text{-}H]^-$. The $[2M\text{-}H]^-$ ion revealed glycitin with an m/z ratio of 891.2362 and an MS/MS fragment at m/z 729.1821 $[C_{18}H_{11}O_5\text{+M+e}]^-$. These components, which were shown to be highly abundant in *U. europaeus* flower, *U. europaeus* stem and *U. dioica*, have been associated with protection against major adverse cardiac events in women [20]. The findings support the use of a plant-based diet and the need for future randomized prospective studies examining the influence of glycitin and genistein, as well as daidzein and dihydrodaidzein diets on cardiovascular outcomes. A literature review on the benefits of phytoestrogen supplementation on human cognition was conflicting, with less than half of the included studies showing beneficial effects, though supplementation with soy isoflavones for less than 6 months, irrespective of dose and mode, can improve cognitive performance, with greater impact on women than men. Equol is seen as an important product of daidzein metabolism in this process, though only 30%–50% of the general population are equol producers. This is thought to affect individual responses to isoflavone intervention [21]. Two isomeric glucosides of daidzein, which are known as daidzin (m/z 397.0933, 3.15 min) and puerarin (m/z 397.0938, 2.97 min), are also a soy isoflavones known to convert to equol. On top of this, identified at a lower score, is *cis*-4-hydroxyequol (m/z 257.0807, 2.32 min) which has activity similar to that of equol itself. Detail is available on glucuronidation via microbial metabolic processes, providing a possible route for how polyphenol glucuronides are formed outside of mammalian metabolism [22,23]. Though the 2 isomers of equol *O*-glucuronide (7 and 4′) were identified at 1.43 and 2.18 min with m/z 417.1198 and m/z 835.2454 parent ions, respectively, literature is scarce on how these two components, found in high amounts in *U. europaeus* stem and flower extracts, would contribute to overall blood plasma equol levels post transformation via gut microbial enzymes.

Naringenin, a flavonoid common in citrus fruits, was found to be another high scoring component, with high abundance in the *U. europaeus* flower and stem extracts. Identified by its $[M\text{-}H]^-$ adduct (m/z 271.0617) at 1.31 min and MS/MS product ion at m/z 243.0654 $[C_{14}H_{12}O_4\text{-}H]^-$, many beneficial biological effects have been linked to naringenin, including antioxidant, cardioprotective, antitumor, antiadipogenic, antiviral, antibacterial and anti-inflammatory effects [24]. In light of the current global pandemic, positive claims have been made as to the therapeutic potential of naringenin in the treatment of COVID-19 [25,26]. Two positional isomers of naringenin were also observed: 3′,4′,7-trihydroxyisoflavanone ($[M\text{-}H_2O\text{-}H]^-$, m/z 253.0518, 1.79 min, dt 2.3328 ms) and 7,3,4-trihydroxyflavanone, also known as butin ($[M\text{-}H]^-$, m/z 271.0604, 1.76 min, dt 2.5498 ms), the former being prominent in *U. europaeus* flower and stem and the latter being of greatest abundance in green tea, but also present in smaller amounts in the other extracts. These had similar retention times but were clearly separated by drift time, and are therefore different molecules. Molecules of this type are often associated with red wine as a contribution from the barrel wood [27] and have been shown to have potential health benefits [28]. In the context of this, naringin, the rhamnoglucoside of naringenin, was likewise identified in *U. europaeus* flowers and stem samples ($[M\text{-}H_2O\text{-}H]^-$, m/z 561.1596, 2.00 min), but at much lower abundance than naringenin. The major confirmatory MS/MS fragment was observed at m/z 515.1190 $[C_{25}H_{26}O_{13}\text{-}H_2O\text{-}H]^-$, showing partial fragmentation of the rhamnoglucoside group. The sugar moiety is a major determinant of the absorption of dietary flavonoid glycosides in mammals [29] and future research into comparative

potency would be of interest here. The identification of naringenin 7-glucuronide ([2M-H]$^-$, *m*/*z* 895.1921, 2.32 min) in high abundance in *U. europaeus* flower extract brings to mind a similar question focused on the potency of the glucuronides of polyphenols.

Tetrahydroxyflavanones have been shown to reduce the heme group in cytochrome c, which is a necessary component of the electron transport system and is also involved in apoptotic pathways. The oxidation state of the iron in the heme group is crucial to its specific functions [30]. These compounds can be seen as the addition of a phenol group to naringenin, with two being observed in these data: 3′,4′,5,7-tetrahydroxyisoflavanone ([2M-H]$^-$, *m*/*z* 575.1184, 1.20 min) and eriodictyol ([M-H]$^-$, *m*/*z* 287.0554, 2.19 min). 3′,4′,5,7-tetrahydroxyisoflavanone was seen significantly only in the reference green tea extract and will therefore receive no further discussion. On the other hand, eriodictyol was present in all of the extracts analysed, with a high abundance in *U. europaeus* flower and stem, but reasonable amounts were also present in *U. dioica* and *A. ursinum* leaf. The potential health benefits of eriodictyol are plentiful [8], with further research showing increasing evidence of its function and benefits. For example, eriodictyol may have therapeutic potential for the treatment of rheumatoid arthritis [31], and a study also shows that eriodictyol may provide a new therapeutic strategy for the management of diabetic retinopathy through the inhibition of high glucose-induced oxidative stress and inflammation in retinal ganglial cells [32].

3′-Hydroxy-O-desmethylangolensin was identified by its [M-H]$^-$ adduct, *m*/*z* 273.0770, at 1.95 min and confirmed by its MS/MS fragment *m*/*z* 119.0497 [C_8H_8O-H]$^-$. This was only seen in significant amounts in the green tea reference and therefore will not be discussed in further detail. This was also the case for 6′-hydroxy-O-desmethylangolensin, which was identified by its [M-H]$^-$ adduct, *m*/*z* 273.0758, at 1.77 min, *p*-hydroxymandelic acid ([M-H]$^-$, *m*/*z* 167.0344, 1.18 min), (−)-epigallocatechin gallate ([M-H_2O-H]$^-$, *m*/*z* 439.0679, 1.76 min), (−)-epicatechin-3-*O*-gallate ([M-H_2O-H]$^-$, *m*/*z* 423.0708, 1.95 min), daidzein 4′-*O*-glucuronide ([M-H_2O-H]$^-$, *m*/*z* 411.0700, 1.42 min) and isopropyl 3-(3,4-dihydroxyphenyl)-2-hydroxypropanoate ([M-H_2O-H]$^-$, *m*/*z* 221.0812, 1.77 min). The strong presence of the heavily documented component of green tea, (−)-epigallocatechin gallate, further validates this discovery workflow [6,27,28]. Furthermore, the product ions *m*/*z* 289.0727 [$C_{15}H_{13}O_6$–H]$^-$, *m*/*z* 169.0146 [$C_7H_5O_5$+e]$^-$ and *m*/*z* 125.0242 [$C_6H_5O_3$+e]$^-$ were consistent with the loss of gallate (169 Da), producing an epigallocatechin minus the C-ring hydroxyl group (289 Da), with further fragmentation causing the loss of the B-ring (125 Da), which was also confirmed by library spectra [33].

Violanone was observed via its [M-H_2O-H]$^-$ adduct, with a score of 55.8 at *m*/*z* 297.0759 and 1.87 min. The main product ion *m*/*z* 121.0282 was due to [$C_7H_6O_2$+e]$^-$. Violanone was predominant in *U. europaeus* flower and stem extracts, but is also an important component of the fragrant Chinese rosewood (*Dalbergia odorifera*), which is used in traditional medicine, with claims broadly relating to its antioxidant qualities [34]. Furthermore, it is shown to selectively inhibit phytopathogenic fungi [35] and to be key component in the roots of *Pongamia pinnata*, which exhibits antioxidant, anticancer, antimicrobial and anti-inflammatory properties through its use in folk medicine [36]. It is noted, too, that the references to violanone in traditional medicinal plants, found in South Asia and China [34–36], also encompass the benefits of many other components identified in these plant extracts from Britain, including daidzein, eriodictyol, naringenin, genistein, isoliquiritigenin ([M-H]$^-$, *m*/*z* 255.0671, 2.72 min) and tectorigenin ([M-H_2O-H]$^-$, *m*/*z* 281.0454, 2.35 min). This begs the question as to whether the published benefits of polyphenols are plant specific, specific to certain phytochemical combinations or specific to a particular molecule in isolation? Isoliquiritigenin is found in very high abundance in *U. europaeus* flower and, to a lesser extent, in *U. europaeus* stem and *S. olusatrum*, with tectorigenin being high in *U. europaeus* stem and lower amounts in *U. europaeus* flower. Isoliquiritigenin is an important bioactive ingredient of traditional Chinese medicine, often extracted from the roots of liquorice plant species, including *Glycyrrhiza uralensis*, *Mongolian glycyrrhiza* and *Glycyrrhiza glabra*, with research exhibiting significant pharmacological properties, includ-

ing both the prevention and treatment of tumours [37]. The transformation of tectoridin ($[M-H]^-$, *m*/*z* 461.1107, 1.55 min), also found in high abundance in *U. europaeus* flower and stem, to the bioactive compound tectorigenin is efficiently achieved by gut microflora, resulting in anaphylaxis inhibitory action [38]. Additionally, recent research suggests that tectorigenin inhibits airway inflammation and pulmonary fibrosis in allergic asthma [39].

4-*O*-Feruloyl-D-quinic acid was identified by its $[M-H]^-$ adduct and parent ion *m*/*z* 367.1050 at 0.43 min. The product ion *m*/*z* 291.0883 was explained by the fragment $[C_{15}H_{16}O_6–H]^-$. 3-Feruloylquinic acid was identified by its $[M-H]^-$ adduct and parent ion *m*/*z* 367.1024 at 1.60 min. The product ion *m*/*z* 295.0802 was explained by the fragment $[C_{14}H_{15}O_7+e]^-$. Chlorogenic acid (3-*O*-Caffeoylquinic acid) was identified by its $[2M-H]^-$ adduct and parent ion *m*/*z* 707.1802 at 2.47 min. The product ions *m*/*z* 663.1927 and *m*/*z* 459.1292 were explained by the fragment $[C_{15}H_{17}O_7+e+M]^-$ and $[C_7H_5O+e+M]^-$, respectively. *p*-Coumaroyl quinic acid was identified by its $[M-H]^-$ adduct and parent ion *m*/*z* 337.0923 at 1.54 min, and the product ion *m*/*z* 307.0820 was explained by the fragment $[C_{15}H_{16}O_7-H]^-$. These four molecules are known as chlorogenic acids, which are a polyphenolic family of quinic acid esters of hydroxyl-cinnamic acids such as *p*-coumaric acid, caffeic acid and ferulic acid. A placebo-controlled double-blind pilot study, conducted in Japan, found that chlorogenic acids decreased arterial stiffness, which is a characteristic of the progression of arteriosclerosis [40]. 4-*O*-Feruloyl-D-quinic acid was found in high amounts in *U. europaeus* flower and *A. ursinum* leaf extracts, whereas 3-feruloylquinic acid was found to be abundant in *S. olusatrum* and *U. dioica*. Chlorogenic acid was found to be most abundant in *U. europaeus* flower and *U. europaeus* stem, with its stereoisomer, neochlorogenic acid, also being observed ($[M-H]^-$, *m*/*z* 353.0876, 1.51 min), which was seen in high abundance in *S. olusatrum* and *U. dioica* as was *p*-coumaroyl quinic acid.

Theaflavin ($[M-H]^-$, *m*/*z* 563.1182, 2.56 min) is created when epicatechin and epigallocatechin come in contact with polyphenol oxidase. This analyte is used as an indicator of production quality in the tea industry, and can be present in low quality green tea but is more common in oolong and black teas. It is shown to be one of many components that are responsible for the antioxidant properties of tea [41]. Here, it is seen in the green tea reference but also in significant abundance in the alexander extract.

The two isomers of procyanidin were identified by their $[M-H]^-$ adduct, one at 1.18 min (*m*/*z* 577.1376) and the other at 1.30 min (*m*/*z* 577.1370), with drift times of 4.5570 ms and 4.6113 ms, respectively. These were either B1, B2, B3 or B4 isomers, but which two could not be determined by the technique as described, although, with external standards of the 4 isomers, retention time and drift time comparison could reveal which is which. Both isomers detected were described by the same three product ions, namely $[C_{22}H_{18}O_9-H]^-$, $[C_{22}H_{16}O_8-H]^-$ and $[C_{15}H_{13}O_6+e]^-$. As expected, these components were dominant in green tea [6,27,28], and both isomers were shown to be present in *U. europaeus* flower and stem extracts. These important phytochemicals, which give rise to the red positively charged cyanidin pigment associated with grapes and berries, exhibit beneficial health effects, including anti-inflammatory, anti-proliferative and antitumor activities, with many reports suggesting procyanidin as a promising lead compound for cancer prevention and treatment [42].

Many glucuronides of potent polyphenols have been identified and, as previously mentioned, most research relates to the creation of these via mammalian metabolism rather than their benefits as a result of ingestion. Of the remaining components, the highlights will be discussed, though further details can be found in the supplementary materials. *U. europaeus* flower extracts were found to have the highest abundance of hesperetin 3′-*O*-glucuronide and genistein 4′-*O*-glucuronide, to name but two examples of many. *U. europaeus* stem had a high abundance of the glucuronide of *cis*-resveratrol [43], which was the component that initially sparked great interest in polyphenols. Additionally, dihydrodaidzein 7-glucuronide was seen with the highest abundance in *U. europaeus* stem. 4′-Methyl epigallocatechin-3′-glucuronide was observed primarily in *U. dioica* extract, although the amount was fairly low. Irisolidone 7-*O*-glucuronide and feruloyl

C1-glucuronide were both seen in very high amounts in *S. olusatrum*, with lower amounts of both being detected in the *A. ursinum* leaf extract.

Benzoic acid (m/z 365.1031, 3.66 min) and salicylic acid (m/z 413.0867, 2.42 min) were both identified via their $[3M-H]^-$ adducts. Benzoic acid was further confirmed by its product ion m/z 347.0926 $[C_7H_5O\text{-}H+2M]^-$, as was the case for salicylic acid MS/MS fragment m/z 369.0980 $[C_6H_5O\text{-}e+2M]^-$. These analytes are commonplace in plants and have been used medicinally for many years, primarily for pain relief and as anti-inflammatory agents [44,45]. These analytes were seen in their highest abundance in *U. europaeus* stem and, to a lesser extent, *U. europaeus* flower. Additionally, *U. dioica* extract contained significant amounts of salicylic acid. Benzoic acid is the functional group in salicylic acid and its derivatives which are responsible for inducing stress tolerance in plants [46].

The high scoring component 5,7-Dihydroxy-8,4′-dimethoxyisoflavone (m/z 329.0660, 2.89 min) is seen as a bioactive component in mung beans (*Vigna radiata*) [47], although very little else is published on this specific methoxyisoflavone. The 2 product ions m/z 311.0552 ($[C_{17}H_{12}O_6\text{-}H]^-$) and m/z 293.0456 ($[C_{17}H_{11}O_5\text{-}H]^-$) helped to confirm the identity of this component. Although its score is high, its abundance is seen to be low across all of the extracts, with small amounts in *U. europaeus* flower and stem. On the other hand, the methoxyisoflavone, irisolidone (m/z 314.0786, 2.69 min), is well documented for health benefits, including anti-helicobacter pylori activity, inhibition of prostaglandin E2 production, hepatoprotective effects, anticancer, estrogenic activity, inhibition of JC-1 virus gene expression and anti-inflammatory activity. Irisolidone is created by the intestinal bacterial transformation of kakkalide (ChemSpider ID 4590337), which is a component of traditional medicine [48]. Irisolidone is evident in good abundance in *U. europaeus* stem and, to a lesser extent, *U. europaeus* flower. The product ion m/z 281.0451 ($[C_{16}H_9O_5\text{+e}]^-$) helped to confirm the identity of irisolidone. Two methoxyisoflavanones (without the double bond on the C-ring) were seen lower on the list of identifications ordered by score. 7,2′-Dihydroxy-4′-methoxyisoflavanone (m/z 267.0663, 2.41 min) and 7-Hydroxy-4′-methoxyisoflavanone (m/z 269.0829, 2.07 min) were seen mainly in *U. europaeus* flower, *U. europaeus* stem and *U. dioica* extracts. 7,2′-Dihydroxy-4′-methoxyisoflavanone has been shown to exist in many plants and is an important component of Tibetan medicine [49]. Isoflavanones are rare compared to isoflavones, with 7-Hydroxy-4′-methoxyisoflavanone being the focus of little research in recent years [50], but it could conceivably have similar activity to its more studied analogues.

The isomers, neohesperidin (m/z 591.1716, 2.77 min) and hesperidin (m/z 591.1724, 2.42 min) were identified with a high score by their $[M\text{-}H_2O\text{-}H]^-$ adducts. These are both derivatives of hesperetin, differing only in the configuration of their rhamnoglucoside moiety and, therefore, cannot, in truth, be specifically identified without external standards, which is made possible due to differences in chromatographic retention times, as well as drift time separation in ion mobility. Hesperidin and derivatives, which are commonly associated with citrus fruits, play an important role in plant defense systems to combat pathogens. It is thought that they may be useful for humans, as they possess antibacterial, antiviral and antifungal activities [51].

Furthermore, hesperidin and derivatives have been shown to have strong activity against the formation of advanced glycation end products which result in the accumulation of random damage in extracellular proteins. This process is known to have deleterious effects on biological functions which are associated with aging and diabetes, such as cataracts, nephropathy, vasculopathy, proliferative retinopathy and atherosclerosis [52]. Large amounts of hesperidin were observed in the *U. europaeus* stem extracts.

Urolithins have been shown to be effective in cancer chemoprevention [53] though, due to differences in gut microbiota, urolithin production capacity from ellagic acid varies amongst individuals [54]. Urolithin C ($[M-H]^-$, m/z 243.0288, 2.15 min) and urolithin A ($[M-H]^-$, m/z 227.0343, 1.75 min) were identified in the extracts studied, with both being significant in *U. europaeus* flowers and urolithin A being noticeably present in *A. ursinum* leaf.

Vanillin is an important flavour and fragrance component in the food industry, and is also used in the pharmaceutical and cosmetic industries. The two components, 3,4-dihydroxybenzadehyde ($[2M-H]^-$, m/z 275.0555, 1.18 min) and vanillic acid ($[3M-H]^-$, m/z 503.1197, 2.35 min), identified in this characterisation of plant extracts, play a key role in the biosynthetic pathway that produces vanillin [55]. 3,4-dihydroxybenzadehyde was found here in good abundance in *U. europaeus* flower, whereas vanillic acid was at its highest abundance in *U. europaeus* stem.

Lignans have been shown to have anticarcinogenic properties. 7-Hydroxymatairesinol has been shown to be effective in a prostate cancer model in vivo [56]. A study in the Netherlands showed that some plant lignans, including 7-hydroxymatairesinol ($[M-H]^-$, m/z 373.1285, 2.32 min), matairesinol ($[M-H]^-$, m/z 357.1336, 2.14 min) and *iso*-lariciresinol ($[M-H]^-$, m/z 359.1499, 1.90 min) can be converted by intestinal microflora into enterolignans, e.g., enterolactone and enterodiol, and may reduce the risk of certain types of cancer, as well as cardiovascular diseases, through anti-oxidant and anti-estrogenic actions [57]. Once again, their highest abundance was to be found in *U. europaeus* flower and stem.

The flavonoid, pseudobaptigenin, can be seen at $[M-H]^-$, m/z 281.0460, 3.10 min and was present in high abundance in *U. europaeus* stem and in lower quantities in *U. europaeus* flower. It is believed that this phytochemical could be used as a prototype for synthesizing new molecules against diabetic cataracts [58]. Although only observed at low abundance in *U. europaeus* stem, 3′,4′,7-trihydroxyisoflavan ($[3M-H]^-$, m/z 773.2626, 2.50 min) was present, but little is published about this trihydroxyisoflavan, which can be produced microbially but is included here for completeness. Found to be high in *S. olusatrum*, 4′,4′′-dimethylepigallocatechin gallate was observed via its $[M-H]^-$ adduct at m/z 485.1076 and 1.46 min. Research shows that methylation of epigallocatechin gallate alters its potency, with a study showing reduced inhibitory effects in macrophages [59], with a further study on cell surface binding abilities showing that dimethylation prevented surface binding completely, suggesting that the hydroxyl groups on the 4′-position in the B ring and the 4′′-position in the gallate are crucial for the cell surface binding activity of epigallocatechin gallate [60].

Finally, we observed three related phytochemicals which all contain the chromone structure and that are very prominent in the polyphenol literature. Firstly, quercetin ($[M-H]^-$, m/z 301.0363, 2.30 min), secondly, isoquercetin ($[M-H_2O-H]^-$, m/z 445.0772, 2.40 min) and, finally, rutin ($[M-H]^-$, m/z 609.1482, 1.43 min). Isoquercetin is quercetin 3-*O*-glucoside and rutin is quercetin 3-*O*-rhamnoglucoside, with the sugar moiety being an important determinant in dietary flavonoid glycosides absorption in humans [29]. Quercetin is present in all the plant samples analysed here, with very high amounts in *U. europaeus* flower and high amounts in *S. olusatrum*. Quercetin is a powerful antioxidant that has a well-documented role in reducing different human cancers, and is one of the most abundant antioxidants in the human diet [61]. In fact, isoquercetin, which was found to be most abundant in *S. olusatrum*, and rutin, which was found in very high amounts in *U. europaeus* flowers, have also been shown to have powerful anti-mutagenic activity [6].

It is noted from a review relating to the drug discovery potential of these components that the chromones of the previous paragraph have large differences in their chemistry and bioactivity compared to the chroman-4-ones, all due to the C_2–C_3 double bond [62]. Naturally occurring chroman-4-ones, such as naringenin, naringin and eriodictyol, were evident in abundance across these plant extracts, providing, together with the other identified polyphenols, a diverse range of bioactivity, with much potential to benefit human and animal health [63].

4. Conclusions

The effective use of UPLC-HDMS^E for the detailed analysis of four common, but low value, green waste materials is demonstrated here. This discovery mode characterisation, which led to the identification of 77 polyphenols with well-documented health potential, opens the door for these plants to provide naturally occurring treatments for disease.

Supplementary Materials: The following are available online at https://www.mdpi.com/article/10.3390/pr9050824/s1. Figure S1: Total ion chromatogram of Alexanders (green) and the alignment reference (magenta), Figure S2: Total ion chromatogram of Gorse Flowers (green) and the alignment reference (magenta), Figure S3: Total ion chromatogram of Gorse Stem (green) and the alignment reference (magenta), Figure S4: Total ion chromatogram of Nettle (green) and the alignment reference (magenta), Figure S5: Total ion chromatogram of Wild Garlic Leaf (green) and the alignment reference (magenta), Figure S6: Total ion chromatogram of Green Tea (green) and the alignment reference (magenta), Figure S7: Molecular structures of identified polyphenolic components, Figure S8: Example mass spectra of identifications ordered from high to low score value, Figure S9: Abundance profile of (−)-epicatechin (CSID65230), *m/z* 289.0732, score 38.1, Figure S10: Alexanders, Smyrnium olusatrum, Figure S11: Stinging Nettle, Urtica dioica, Figure S12: Wild garlic, Allium ursinum, Figure S13: Gorse, Ulex europaeus, Green Waste extracts XL SM v7 is a spreadsheet of identifications and abundances.

Author Contributions: This research was conceptualized by C.M.P., who was also responsible for methodology and formal analysis. The samples were collected, prepared and analysed by C.M.P. The first draft of this manuscript was written by C.M.P. and reviewed and edited by D.L.J. and C.M.P. All authors have read and agreed to the published version of the manuscript.

Funding: This research received no external funding.

Institutional Review Board Statement: Not applicable.

Informed Consent Statement: Not applicable.

Data Availability Statement: Data available on request.

Acknowledgments: The authors are highly appreciative to the Welsh European Funding Office (WEFO) in respect to their funding of the Centre for Environmental Technology at Bangor University. The excellent assistance of E.S. Potter is acknowledged for the creation of the heat map.

Conflicts of Interest: The authors declare that they have no known competing financial interests or personal relationships that could have appeared to influence the work reported in this paper.

References

1. Sheldon, R.A. Green and sustainable manufacture of chemicals from biomass: State of the art. *Green Chem.* **2014**, *16*, 950–963. [CrossRef]
2. Langsdorf, A.; Volkmar, M.; Holtmann, D.; Ulber, R. Material utilization of green waste: A review on potential valorization methods. *Bioresourc Bioprocess.* **2021**, *8*, 19. [CrossRef]
3. Barba, F.J.; Zhu, Z.Z.; Koubaa, M.; Sant'Ana, A.S.; Orlien, V. Green alternative methods for the extraction of antioxidant bioactive compounds from winery wastes and by-products: A review. *Trends Food Sci. Technol.* **2016**, *49*, 96–109. [CrossRef]
4. De La Iglesia, R.; Milagro, F.I.; Campión, J.; Boqué, N.; Martínez, J.A. Healthy properties of proanthocyanidins. *BioFactors* **2010**, *36*, 159–168. [CrossRef]
5. Krikorian, R.; Kalt, W.; Mcdonald, J.E.; Shidler, M.D.; Summer, S.S.; Stein, A.L. Cognitive performance in relation to urinary anthocyanins and their flavonoid-based products following blueberry supplementation in older adults at risk for dementia. *J. Funct. Foods* **2019**, 103667. [CrossRef]
6. Preedy, V.; Zibadi, S.; Watson, R. *Polyphenols in Human Health and Disease*; Academic Press: New York, NY, USA, 2014; Volume 1, ISBN 9780123984562.
7. Uyama, H.; Kobayashi, S. Enzymatic synthesis of polyphenols. *Curr. Org. Chem.* **2003**, *7*, 1387–1397. [CrossRef]
8. Potter, C.M.; Jones, D.L. Polyphenolic Profiling of Forestry Waste by UPLC-HDMSe. *Processes* **2020**, *8*, 1411. [CrossRef]
9. Wu, F.F.; Sun, H.; Wei, W.F.; Han, Y.; Wang, P.; Dong, T.W.; Yan, G.L.; Wang, X.J. Rapid and global detection and characterization of the constituents in ShengMai San by ultra-performance liquid chromatography-high-definition mass spectrometry. *J. Sep. Sci.* **2011**, *34*, 3194–3199. [CrossRef]
10. Wang, P.; Sun, H.; Lv, H.; Sun, W.; Yuan, Y.; Han, Y.; Wang, D.W.; Zhang, A.H.; Wang, X.J. Thyroxine and reserpine-induced changes in metabolic profiles of rat urine and the therapeutic effect of Liu Wei Di Huang Wan detected by UPLC-HDMS. *J. Pharm. Biomed. Anal.* **2010**, *53*, 631–645. [CrossRef]
11. Da Silva Pinto, M. Tea: A new perspective on health benefits. *Food Res. Int.* **2013**, *53*, 558–567. [CrossRef]
12. Sapozhnikova, Y. Development of liquid chromatography-tandem mass spectrometry method for analysis of polyphenolic compounds in liquid samples of grape juice, green tea and coffee. *Food Chem.* **2014**, *150*, 87–93. [CrossRef]
13. Vos, F.; Crespy, V.; Chaffaut, L.; Mennen, L.; Knox, C.; Neveu, V. Phenol-Explorer: An online comprehensive database on polyphenol contents in foods. *Database* **2010**, *2010*, 1–9. [CrossRef]

14. Pandey, R.; Chandra, P.; Arya, K.R.; Kumar, B. Development and validation of an ultra high performance liquid chromatography electrospray ionization tandem mass spectrometry method for the simultaneous determination of selected flavonoids in Ginkgo biloba. *J. Sep. Sci.* **2014**, *37*, 3610–3618. [CrossRef]
15. Lopes, N.P.; Demarque, D.P.; Crotti, A.E.M.; Vessecchi, R.; Lopes, J. Fragmentation reactions using electrospray ionization mass spectrometry: An important tool for the structural elucidation and characterization of synthetic and natural products. *RSC-Nat. Prod. Rep.* **2016**, *33*, 432. [CrossRef]
16. Ahn, H.J.; You, J.; Park, S.; Li, Z.; Choe, D. RSC Advances and their contribution to improved anti-inflammatory activity. *RSC Adv.* **2020**, *10*, 5339–5350. [CrossRef]
17. Chaitanya, M.V.N.L.; Suresh, P.; Dhanabal, P.; Jubie, S. Human Topopoisons From Weeds: A Review. *Curr. Tradit. Med.* **2018**, *4*, 4–15. [CrossRef]
18. Andersen Oyvind, M.; Dersen Markham, K.R. *Flavonoids: Chemistry, Biochemistry and Applications*; CRC Press: Boca Raton, FL, USA, 2006; Volume 45, ISBN 9780849320217.
19. Gülçin, I. Antioxidant activity of caffeic acid (3,4-dihydroxycinnamic acid). *Toxicology* **2006**, *217*, 213–220. [CrossRef] [PubMed]
20. Barsky, L.; Cook-Wiens, G.; Doyle, M.; Shufelt, C.; Rogers, W.; Reis, S.; Pepine, C.J.; Noel Bairey Merz, C. Phytoestrogen blood levels and adverse outcomes in women with suspected ischemic heart disease. *Eur. J. Clin. Nutr.* **2020**. [CrossRef] [PubMed]
21. Zaw, J.J.T.; Howe, P.R.C.; Wong, R.H.X. Does phytoestrogen supplementation improve cognition in humans? A systematic review. *Ann. N. Y. Acad. Sci.* **2017**, *1403*, 150–163. [CrossRef]
22. Costa, E.M.D.M.B.; Pimenta, F.C.; Luz, W.C.; De Oliveira, V. Selection of filamentous fungi of the Beauveria genus able to metabolize quercetin like mammalian cells. *Braz. J. Microbiol.* **2008**, *39*, 405–408. [CrossRef]
23. Marvalin, C.; Azerad, R. Microbial glucuronidation of polyphenols. *J. Mol. Catal. B Enzym.* **2011**, *73*, 43–52. [CrossRef]
24. Salehi, B.; Fokou, P.V.T.; Sharifi-Rad, M.; Zucca, P.; Pezzani, R.; Martins, N.; Sharifi-Rad, J. The therapeutic potential of naringenin: A review of clinical trials. *Pharmaceuticals* **2019**, *12*, 11. [CrossRef] [PubMed]
25. Tutunchi, H.; Naeini, F.; Ostadrahimi, A.; Hosseinzadeh-Attar, M.J. Naringenin, a flavanone with antiviral and anti-inflammatory effects: A promising treatment strategy against COVID-19. *Phyther. Res.* **2020**, *1*, 1–11. [CrossRef]
26. Alberca, R.W.; Teixeira, F.M.E.; Beserra, D.R.; de Oliveira, E.A.; de Andrade, M.M.S.; Pietrobon, A.J.; Sato, M.N. Perspective: The Potential Effects of Naringenin in COVID-19. *Front. Immunol.* **2020**, *11*, 1–9. [CrossRef] [PubMed]
27. Sanz, M.; Fernández de Simón, B.; Esteruelas, E.; Muñoz, Á.M.; Cadahía, E.; Hernández, M.T.; Estrella, I.; Martinez, J. Polyphenols in red wine aged in acacia (Robinia pseudoacacia) and oak (Quercus petraea) wood barrels. *Anal. Chim. Acta* **2012**, *732*, 83–90. [CrossRef]
28. Duan, J.; Guan, Y.; Mu, F.; Guo, C.; Zhang, E.; Yin, Y.; Wei, G.; Zhu, Y.; Cui, J.; Cao, J.; et al. Protective effect of butin against ischemia/reperfusion-induced myocardial injury in diabetic mice: Involvement of the AMPK/GSK-3β/Nrf2 signaling pathway. *Sci. Rep.* **2017**, *7*, 1–14. [CrossRef] [PubMed]
29. Hollman, P.C.H.; Bijsman, M.N.C.P.; Van Gameren, Y.; Cnossen, E.P.J.; De Vries, J.H.M.; Katan, M.B. The sugar moiety is a major determinant of the absorption of dietary flavonoid glycosides in man. *Free Radic. Res.* **1999**, *31*, 569–573. [CrossRef]
30. Rabago Smith, M.; Kindl, E.D.; Williams, I.R.; Moorman, V.R. 5,7,3′,4′-Hydroxy substituted flavonoids reduce the heme of cytochrome c with a range of rate constants. *Biochimie* **2019**, *162*, 167–175. [CrossRef]
31. Liu, Y.C.; Yan, X.N. Eriodictyol inhibits survival and inflammatory responses and promotes apoptosis in rheumatoid arthritis fibroblast-like synoviocytes through AKT/FOXO1 signaling. *J. Cell. Biochem.* **2019**, *120*, 14628–14635. [CrossRef]
32. Lv, P.; Yu, J.; Xu, X.; Lu, T.; Xu, F. Eriodictyol inhibits high glucose-induced oxidative stress and inflammation in retinal ganglial cells. *J. Cell. Biochem.* **2019**, *120*, 5644–5651. [CrossRef]
33. HighChem LLC mzCloud. Available online: https://www.mzcloud.org/ (accessed on 1 December 2020).
34. The, S.N. A Review on the Medicinal Plant Dalbergia odorifera Species: Phytochemistry and Biological Activity. *Evid.-Based Complement. Altern. Med.* **2017**, *1*. [CrossRef]
35. Deesamer, S.; Kokpol, U.; Chavasiri, W.; Douillard, S.; Peyrot, V.; Vidal, N.; Combes, S.; Finet, J.P. Synthesis and biological evaluation of isoflavone analogues from Dalbergia oliveri. *Tetrahedron* **2007**, *63*, 12986–12993. [CrossRef]
36. Wen, R.; Lv, H.; Jiang, Y.; Tu, P. Anti-inflammatory isoflavones and isoflavanones from the roots of *Pongamia pinnata* (L.) Pierre. *Bioorganic Med. Chem. Lett.* **2018**, *28*, 1050–1055. [CrossRef]
37. Peng, F.; Du, Q.; Peng, C.; Wang, N.; Tang, H.; Xie, X.; Shen, J.; Chen, J. A Review: The Pharmacology of Isoliquiritigenin. *Phyther. Res.* **2015**, *29*, 969–977. [CrossRef]
38. Park, E.-K.; Shin, Y.-W.; Lee, H.-U.; Lee, C.S.; Kim, D. Passive Cutaneous Anaphylaxis-Inhibitory Action of Tectorigenin, a Metabolite of Tectridin by Intestinal Microflora. *Biol. Pharm. Bull.* **2004**, *27*, 1099–1102. [CrossRef] [PubMed]
39. Wang, Y.; Jing, W.; Qu, W.; Liu, Z.; Zhang, D.; Qi, X.; Liu, L. Tectorigenin inhibits inflammation and pulmonary fibrosis in allergic asthma model of ovalbumin-sensitized guinea pigs. *J. Pharm. Pharmacol.* **2020**, *72*, 956–968. [CrossRef] [PubMed]
40. Suzuki, A.; Nomura, T.; Jokura, H.; Kitamura, N.; Saiki, A.; Fujii, A. Chlorogenic acid-enriched green coffee bean extract affects arterial stiffness assessed by the cardio-ankle vascular index in healthy men: A pilot study. *Int. J. Food Sci. Nutr.* **2019**, *70*, 901–908. [CrossRef]
41. Drynan, J.W.; Clifford, M.N.; Obuchowicz, J.; Kuhnert, N. The chemistry of low molecular weight black tea polyphenols. *Nat. Prod. Rep.* **2010**, *27*, 417–462. [CrossRef] [PubMed]
42. Lee, Y. Cancer chemopreventive potential of procyanidin. *Toxicol. Res.* **2017**, *33*, 273–282. [CrossRef]

43. Wiciski, M.; Leis, K.; Szyperski, P.; Ę Eclewicz, M.M.; Mazur, E.; Pawlak-Osiska, K. ARTICLE IN PRESS Impact of resveratrol on exercise performance: A review Effet du resveratrol sur la performance physique: Revue générale. *Sci. Sport.* **2018**, *1*. [CrossRef]
44. Qualley, A.V.; Widhalm, J.R.; Adebesin, F.; Kish, C.M.; Dudareva, N. Completion of the core β-oxidative pathway of benzoic acid biosynthesis in plants. *Proc. Natl. Acad. Sci. USA* **2012**, *109*, 16383–16388. [CrossRef]
45. Raskin, I. Role of salicylic acid in plants. *Annu. Rev. Plant Physiol. Plant Mol. Biol.* **1992**, *43*, 439–463. [CrossRef]
46. Senaratna, T.; Merritt, D.; Dixon, K.; Bunn, E.; Touchell, D.; Sivasithamparam, K. Benzoic acid may act as the functional group in salicylic acid and derivatives in the induction of multiple stress tolerance in plants. *Plant Growth Regul.* **2003**, *39*, 77–81. [CrossRef]
47. Ganesan, K.; Xu, B. A critical review on phytochemical profile and health promoting effects of mung bean (Vigna radiata). *Food Sci. Hum. Wellness* **2018**, *7*, 11–33. [CrossRef]
48. Kang, K.A.; Zhang, R.; Piao, M.J.; Ko, D.O.; Wang, Z.H.; Kim, B.J.; Park, J.W.; Kim, H.S.; Kim, D.H.; Hyun, J.W. Protective effect of irisolidone, a metabolite of kakkalide, against hydrogen peroxide induced cell damage via antioxidant effect. *Bioorganic Med. Chem.* **2008**, *16*, 1133–1141. [CrossRef] [PubMed]
49. Wang, Q.; Wu, X.; Yang, X.; Zhang, Y.; Wang, L.; Li, X.; Qiu, Y. Comprehensive quality evaluation of Lignum Caraganae and rapid discrimination of Caragana jubata and Caragana changduensis based on characteristic compound fingerprints by HPLC-UV and HPLC-MS/MS coupled with chemometrics analysis. *Phytochem. Anal.* **2020**, *31*, 846–860. [CrossRef]
50. Al-Maharik, N. Isolation of naturally occurring novel isoflavonoids: An update. *Nat. Prod. Rep.* **2019**, *36*, 1156–1195. [CrossRef]
51. Iranshahi, M.; Rezaee, R.; Parhiz, H.; Roohbakhsh, A.; Soltani, F. Protective effects of flavonoids against microbes and toxins: The cases of hesperidin and hesperetin. *Life Sci.* **2015**, *137*, 125–132. [CrossRef]
52. Li, D.; Mitsuhashi, S.; Ubukata, M. Protective effects of hesperidin derivatives and their stereoisomers against advanced glycation end-products formation. *Pharm. Biol.* **2012**, *50*, 1531–1535. [CrossRef] [PubMed]
53. Stanisławska, I.J.; Piwowarski, J.P.; Granica, S.; Kiss, A.K. The effects of urolithins on the response of prostate cancer cells to non-steroidal antiandrogen bicalutamide. *Phytomedicine* **2018**, *1*. [CrossRef]
54. García-Villalba, R.; Beltrán, D.; Espín, J.C.; Selma, M.V.; Tomás-Barberán, F.A. Time course production of urolithins from ellagic acid by human gut microbiota. *J. Agric. Food Chem.* **2013**, *61*, 8797–8806. [CrossRef]
55. Kundu, A. Vanillin biosynthetic pathways in plants. *Planta* **2017**, *245*, 1069–1078. [CrossRef]
56. Bylund, A.; Saarinen, N.; Zhang, J.X.; Bergh, A.; Widmark, A.; Johansson, A.; Lundin, E.; Adlercreutz, H.; Hallmans, G.; Stattin, P.; et al. Anticancer effects of a plant lignan 7-hydroxymatairesinol on a prostate cancer model in vivo. *Urol. Oncol. Semin. Orig. Investig.* **2005**, *23*, 380–381. [CrossRef]
57. Milder, I.E.J.; Feskens, E.J.M.; Arts, I.C.W.; De Mesquita, H.B.B.; Hollman, P.C.H.; Kromhout, D. Intake of the Plant Lignans Secoisolariciresinol, Matairesinol, Lariciresinol, and Pinoresinol in Dutch Men and Women 1. *Nutr. Epidemiol.* **2005**, *135*, 1202–1207. [CrossRef] [PubMed]
58. Jeevanandam, J.; Madhumitha, R.; Saraswathi, N.T. Identification of potential phytochemical lead against diabetic cataract: An in silico approach. *J. Mol. Struct.* **2020**, *1226*, 129428. [CrossRef]
59. Chiu, F.L.; Lin, J.K. HPLC analysis of naturally occurring methylated catechins, 3″- and 4″-methyl-epigallocatechin gallate, in various fresh tea leaves and commercial teas and their potent inhibitory effects on inducible nitric oxide synthase in macrophages. *J. Agric. Food Chem.* **2005**, *53*, 7035–7042. [CrossRef]
60. Yano, S.; Fujimura, Y.; Umeda, D.; Miyase, T.; Yamada, K.; Tachibana, H. Relationship between the biological activities of methylated derivatives of (-)-epigallocatechin-3-O-gallate (EGCG) and their cell surface binding activities. *J. Agric. Food Chem.* **2007**, *55*, 7144–7148. [CrossRef]
61. Rauf, A.; Imran, M.; Khan, I.A.; ur-Rehman, M.; Gilani, S.A.; Mehmood, Z.; Mubarak, M.S. Anticancer potential of quercetin: A comprehensive review. *Phyther. Res.* **2018**, *32*, 2109–2130. [CrossRef] [PubMed]
62. Emami, S.; Ghanbarimasir, Z. Recent advances of chroman-4-one derivatives: Synthetic approaches and bioactivities. *Eur. J. Med. Chem.* **2015**, *93*, 539–563. [CrossRef]
63. Shyamal, K.; Jash, G.B. Recent progress in the research of naturally occurring flavonoids: A look through. *Signpost Open Access J. Org. Biomol. Chem.* **2013**, *1*, 65–168.